Scaled-Energy Spectroscopy of the Rydberg-Stark Spectrum of Helium: Influence of Exchange on Recurrence Spectra

M. Keeler and T. J. Morgan

Department of Physics, Wesleyan University, Middletown, Connecticut 06459

(Received 4 December 1997)

We report the first observation of the manifestation of exchange effects in recurrence spectra. Using fast-atom–laser-beam scaled-energy spectroscopy, we have measured the Rydberg-Stark recurrence spectrum of the two spin forms of helium in strong fields. Singlets and triplets are produced by excitation of metastable $1s2s\,^{1,3}S$ states. We observe pronounced modulations in the triplet spectrum due to interference between hydrogenic and core-scattered combination orbits. The modulations are phase correlated with repeating hydrogenic orbits and not present in singlets or in hydrogen. [S0031-9007(98)06521-1]

PACS numbers: 32.60.+i, 03.65.Sq

A complete theoretical treatment of nonhydrogenic atoms in external fields remains a challenge. Experimental progress has provided substantial information on Rydberg atoms in external fields [1]. Application of the semiclassical description, in the form of closed orbit theory, has been quite successful and is the basis for the field of recurrence spectroscopy [2]. Standard closed orbit theory treats nonhydrogenic effects with quantum defects. Recently, nonhydrogenic effects have been included through core-scattered waves [3] and by an explicit core potential resulting in classical core scattering [4]. These extensions have demonstrated that core scattering gives rise to combination orbits not seen in hydrogen. To date, experimental studies of Rydberg-Stark recurrence spectra have used alkali atoms which contain closed shell ionic cores and have one spin state [5,6]. The present work extends experiment to open shell ionic cores and their role in producing combination orbits. In addition, open shell cores provide polarized spin-state dependent scattering systems that permit experimental access to the influence of electron exchange.

The exchange interaction is isolated experimentally by measuring recurrence spectra versus spin state. This provides a tool to examine the role of the Pauli exclusion principle in the semiclassical theory and in the dynamics of Rydberg systems, where it is not well understood. Closed orbits are sensitive to the spin-dependent exchange interaction since the Rydberg electron returns to the nucleus and the charge clouds of the electrons overlap. In helium, when the Rydberg electron samples the core, it moves as if it experiences an attraction or repulsion depending on the relative orientation of the two spins. This introduces a coupling between the spatial variables of the Rydberg electron and the spin state of the atom. How this is revealed in the Stark recurrence spectrum of the prototypical two-electron helium atom is a focus of the present Letter.

Extensive data have been obtained for $m = 1$ states at 60 different scaled energies in strong fields ($20 < n < 30$) up to scaled action 15. This allows a global view of the spectrum and observation of trajectory evolution as a function of scaled energy. Using this information, we introduce a new analysis technique of integrating recurrence strength of an orbit over its scaled energy range. This permits study of the behavior of orbit types independent of launching angle, and that occur at very different scaled energies.

In our experiment the absorption spectrum is measured at fixed scaled energy $\varepsilon = EF^{-1/2}$ over a range of n, where F is the applied electric field strength and E the total energy of the electron. In this case, the classical Hamiltonian of the system is not dependent on the energy of the electron and electric field separately, but rather on scaled energy only [2]. Recording spectra at fixed scaled energy maintains the same classical dynamics at all points in the spectrum.

The physical picture associated with recurrence spectroscopy is based on closed orbit theory [2]. When a photon is absorbed by an atom in an electric field, the electron becomes a near-zero-energy Coulomb outgoing wave. After sufficient distance, the wave propagates semiclassically and follows classical trajectories. Trajectories that are turned back by the combined Coulomb and external electric field eventually become waves that interfere with outgoing waves provided they return near the nucleus. This "atomic interferometer" gives structure to the photoabsorption spectrum.

It can be shown from closed orbit theory that the average oscillator strength density is

$$Df(\varepsilon, F) = Df_0 + \sum_k \sum_j C_{k,j}(\varepsilon) \sin(2\pi j \hat{S}_k F^{-1/4} - \alpha_{k,j}), \tag{1}$$

where

$$\alpha_{k,j} = j\left[\frac{\pi}{2}\,\mu^k + \frac{3}{2}\,\pi\right] - \frac{3\pi}{4} - \Delta_k\,. \tag{2}$$

Df_0 is the flat background when the electric field is not present. This semiclassical result is exact for hydrogen

 0031-9007/98/80(26)/5726(4)$15.00

and a good approximation for other Rydberg systems. It applies to all orbits that are not on the field axis. We neglect those on axis because of the centrifugal barrier for $m = 1$ states. The second term is a sum over all closed orbits k, including repetitions j. $C_{k,j}(\varepsilon)$ is the recurrence amplitude and its square the recurrence strength. It incorporates trajectory stability, the geometry of a transition, and the quantum defect. The sinusoidal part arises from phase differences between outgoing and returning waves and is described by the classical scaled action $\hat{S}_k$ adjusted by a constant $\alpha_{k,j}$. μ^k is the Maslov index and Δ_k is the phase shift caused by the core and is related to the quantum defect. $\Delta_k = 0$ for hydrogen. Each closed orbit provides a sinusoidal variation to the scaled absorption spectrum. Consequently, the Fourier transform power spectrum with respect to $F^{-1/4}$, referred to as the recurrence spectrum, yields discrete peaks at scaled actions of classical closed orbits, their repetitions, and their combinations. The amplitude of a peak at a scaled action is the coherent sum of orbit contributions to that action within experimental resolution. Combination orbits are created by scattering of one orbit into another by the core and do not exist in hydrogen. The action of combination orbits is approximately the sum of the constituent hydrogen orbits.

Nonhydrogenic effects are incorporated within closed orbit theory through quantum defects, affecting the amplitude and phase of a classical closed orbit [2]. Neglecting relativistic effects, the quantum defect for helium separates into two parts $\delta = \delta_c \pm \delta_{\rm ex}$: one from electron exchange $\pm\delta_{\rm ex}$ and a direct Coulomb part δ_c, identical for both spin states, due to screening and polarization [7]. The spin dependence of the quantum defect is contained in the $\pm$ sign: $+$ for triplets, $-$ for singlets. This term, due to the requirement of antisymmetrization of the total wave function imposed by the Pauli exclusion principle, is responsible for spin-dependent effects in our recurrence spectra. $\delta_{\rm ex} = 0$, to first order, for alkali atoms. Since $1 \geq m$ there is no s-state character in our spectra and the main contribution to the quantum defect comes from the p-state quantum defect, which is dominated by $\delta_{\rm ex}$. This is seen in Table I, where we list relevant quantum defects for helium.

Figure 1 shows the experiment. A beam of metastable $1s2s\,^{1,3}S$ helium atoms is prepared by starting with a He^+ beam. Ions are produced in an ion source, extracted, focused, accelerated to 4 keV, and passed through a velocity filter. The ion beam undergoes near-resonant charge transfer collisions in a potassium vapor cell. The metastable states formed have long lifetimes compared to their transit time. Ions that do not undergo charge transfer are removed from the beam by an electric field and monitored. The beam of metastables enters a 37-cm drift region that contains an electric field transverse to it, produced by a pair of plates separated by 1.0 cm. In this region the metastables are excited to Stark-Rydberg states by a counterpropagating collinear 20-Hz uv dye-laser beam produced by frequency doubling the output of a Nd:YAG-pumped dye laser. Excitation energy below zero-field ionization limit ranged from 274.18 to 121.84 $\rm cm^{-1}$. Each constant scaled-energy spectrum covers 52.34 $\rm cm^{-1}$, and was recorded in a continuous scan lasting $\sim$15 min. The range of applied field was 130 V $\rm cm^{-1}$ to 2168 V $\rm cm^{-1}$. Linearly polarized light was oriented perpendicular to the field, exciting $m = 1$ states.

TABLE I. $l = 0$, 1 quantum defects for triplet and singlet helium.

l	δ_c	$\delta_{\rm ex}$	$\delta_{\rm trip}$	$\delta_{\rm sing}$
0	0.22	0.08	0.30	0.14
1	0.03	0.04	0.07	−0.01

After the interaction region the beam enters a field ionizer of 7.0 kV $\rm cm^{-1}$, oriented along the beam axis, that ionizes Rydberg atoms and accelerates resulting He^+ ions into an analyzer for detection by a channeltron. The modulated ion signal is amplified, boxcar averaged, and recorded. To maintain a fixed scale energy $\varepsilon = EF^{-1/2}$, the computer monitors the laser wavelength and adjusts the electric field, while recording data. For a fixed scaled energy, spectral data are recorded as a function of $F^{-1/4}$ and a Fourier transform is applied to obtain the recurrence spectrum.

Contributions to uncertainty in scaled energy arise from knowledge of electric field strength and laser energy. The applied voltage is accurate to $<1\%$, and spacing between field plates is known to $\sim 10^{-3}$ cm. Laser wavelength is calibrated from field free spectra. Uncertainty in wavelength is due primarily to reproducibility of a wavelength setting, accurate to <0.04 $\rm cm^{-1}$. These effects conspire to produce an uncertainty in the value of scaled energy of about 0.2%. Laser linewidth is about 0.4 $\rm cm^{-1}$.

Recurrence spectra have been measured for singlet and triplet helium for scaled energy from -2.0 (classical ionization threshold) to -3.5, and up to $\hat{S} = 15$, with $\Delta\hat{S} = \sim 0.1$. In Fig. 2 we present an experimental triplet recurrence map. Three sequences of peaks are identified

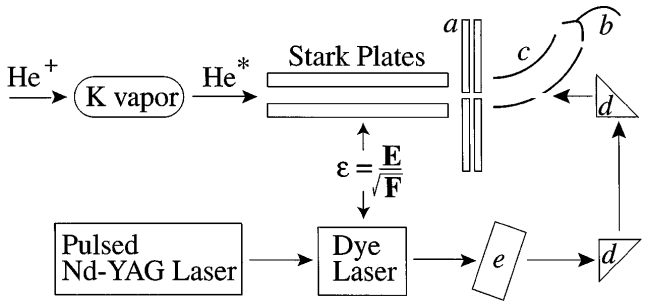

FIG. 1. Experiment: (a) ionizer, (b) channeltron, (c) deflector, (d) prisms, and (e) doubler. The scaling $\varepsilon = EF^{-1/2}$ between Stark plates and dye laser is shown.

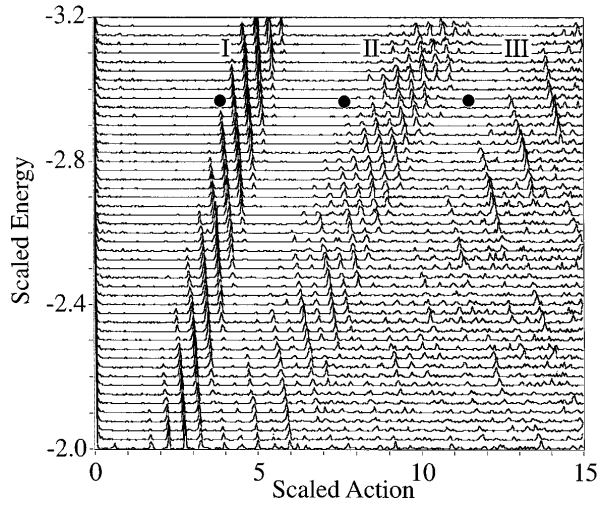

FIG. 2. Experimental recurrence map of Rydberg-Stark spectrum of $m = 1$ triplet helium. I, II, and III indicate the classical closed orbit sequences. Solid dots are above the $\frac{9}{10}$ orbit and its repetitions.

cutting through the map at different angles, labeled I, II, and III. In hydrogen, the sequences result from individual orbits and their repetitions, and are classified [2,5] into types according to their period ratios τ_u/τ_v in semiparabolic coordinates where $u = (r + z)^{1/2}$ and $v = (r - z)^{1/2}$. Sequences I, II, and III correspond to $\tau_u/\tau_v = i/i + 1$, $i/i + 2$, $i/i + 3$, with i an integer. Sequence II orbits consist of two alternating types: irreducible nonrepeating orbits and reducible repeating orbits. A sequence II reducible orbit, for example, $\frac{12}{14}$, repeats sequence I $\frac{6}{7}$ orbit two times. Sequence III consists of reducible and irreducible orbits also, with reducible orbits repeating I orbits three times and separated by two irreducible orbits.

For $m = 1$ helium, the Stark structure should look hydrogenic. We find this to be true; however, two of the hydrogen recurrence sequences (II and III) are modified, containing modulations in peak strength not present in hydrogen. Recent experimental work on the Stark structure of lithium found nonhydrogenic behavior in $m = 0$ states, identifying new peaks in the spectrum at locations far from hydrogen, and due to combination orbits from core scattering [5]. In the present case combination orbits occur very close to hydrogenic peaks, modifying the hydrogenic spectra because of interference and producing the novel structure shown in Fig. 2. Combination orbits in II arise from two different orbit pairs in I. Combination orbits that interfere with repeating $i/i + 1 \times 2$ hydrogen orbits are $i - 1/i \oplus i + 1/i + 2$ and $i - 2/i - 1 \oplus i + 2/i + 3$, where $\oplus$ indicates [4] core scattering from one hydrogenic orbit into another. For example, at $\varepsilon = -2.7$, the $2 \times \frac{9}{10}$ orbit recurs at $\hat{S}_k = 8.187$ and interferes with the $\frac{8}{9} \oplus \frac{10}{11}$ orbit recurring at $\hat{S}_k = 8.177$ and the $\frac{7}{8} \oplus \frac{11}{12}$ orbit at $\hat{S}_k = 8.149$. Combination orbits in III are more complex and come from both I and II, with double core scattering possible. Changes in the spectrum due to the presence of interloping combination orbits are dramatic in the triplet case, introducing a strong peak height modulation in sequences II and III as seen in Fig. 2 (see also Fig. 3).

We examine the data of Fig. 2 using a new recurrence spectroscopy analysis technique. Rather than comparing results at fixed scaled energy, which provides only a local view of an orbit at a specific launching angle, we focus on global properties, independent of launching angle, by integrating recurrence strength in each constituent orbit of a particular type. This allows identification of spin-state-dependent behavior in terms of hydrogenic orbit types, and comparison of orbits that do not exist at the same scaled energy. In Fig. 3 we present total strength of II (III) orbits versus hydrogen-orbit period ratio τ_u/τ_v, with two (three) time repeating orbits indicated by arrows. Also shown is the result of a simple quantum hydrogen

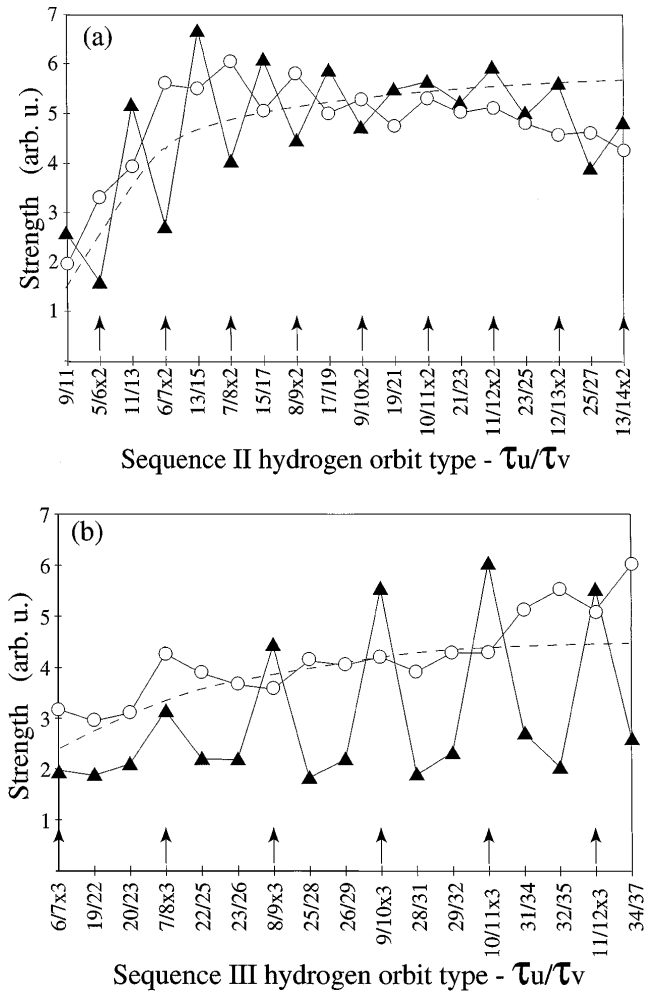

FIG. 3. Integrated experimental recurrence strength versus hydrogen orbit type. Arrows indicate repeating orbits. Closed triangles: triplet helium; open circles: singlet helium. Hydrogen calculation is shown as a dashed line. (a) Sequence II. (b) Sequence III. Vertical scales are the same.

calculation [8], normalized at the recurrence strength of the singlet $\frac{9}{10}$ repeating orbit, included to show lack of any modulation in hydrogen. This figure reveals the recurrence strength's dramatic dependence on spin state. Overall, singlets and hydrogen behave similarly. In the triplet case strong modulation in recurrence strength is present in both sequences. In II, triplet primitive (repeating) orbit recurrence strength is favored at lower (higher) scaled action. In III, triplet modulation grows in strength with repeating orbits always favored.

The origin of the selectivity to hydrogenic orbit type (primitive or repeating) of the modulations can be explained within the context of closed orbit theory. In the vicinity of a hydrogenic recurrence peak there are several combination orbit peaks. The phase of the interference is equal to $2\pi F^{-1/4}\Delta\hat{S}$, where $F^{-1/4}$ is the average value of the scaled variable and $\Delta\hat{S}$ is the scaled-action distance between peaks. Orbit calculations indicate that $\Delta\hat{S}$ is usually very small, of order 0.01. However, since the value of $F^{-1/4}$ is proportional to n, it has a considerable value, about 60, so the total phase shift can be of order π. The closer a combination recurrence is to a hydrogenic peak, the smaller the phase of the interference. Consequently, the main cause of the observed interference effects in the recurrence spectrum is contained in $\Delta\hat{S}$. It turns out that $\Delta\hat{S}$ has a regular pattern which depends on (i) the hydrogenic orbit type (primitive or repeating) and (ii) the recurrence sequence (type II or III orbits). Inspection shows that clusters of nearby combination peaks are much closer to primitive hydrogenic orbits than to repeating ones and have a regular dependence of the minimal distance between hydrogenic and combination peaks on the type of hydrogenic orbit. Denoting $\Delta\hat{S} = d$ as the shortest distance between repeating and combination orbits in sequence II, it can be shown [9] that this distance in sequence III is $(\frac{3}{4})d$, and that the comparable distances for primitive orbits are $(\frac{1}{4})d$ and $(\frac{1}{12})d$. It is the regular nature of the separations $\Delta\hat{S}$ that produce oscillations which correlate with hydrogenic orbits. The amplitude of the oscillations can be estimated with the aid of scattering theory as Abs $(e^{2\pi i\mu} - 1)^2 \sim 4\pi^2\mu^2 = 0.19$, for a quantum defect $\mu = 0.07$. This value is in accord with our measurements, which vary between 20% and 50% (see Fig. 3), since several combination orbits interfere with different phases. A detailed closed orbit theory calculation of the experimentally observed modulations must include explicit phase counting of all relevant combination orbits and integration over a range of scaled energy. A thorough theoretical analysis of this type will be addressed in a future paper.

A recent theoretical Letter [10] on diffractive orbits of Rydberg atoms in external fields provides new insight into the classical interpretation of quantum defects. Our work provides stimulus for investigation of the classical interpretation of the exchange interaction and illuminates this intriguing aspect of classical-quantum correspondence.

In summary, the measurement of different spin states in our experiment demonstrates the influence of exchange on recurrence spectra. We observe two main effects: (i) pronounced modulation in the recurrence map of triplet helium, not present in singlet helium nor in hydrogen, and (ii) strong phase correlation of the modulation with repeating hydrogenic orbits, producing suppression of recurrence strength in second repetitions and enhancement of strength in third repetitions. These effects result from the interference between hydrogenic orbits and core-scattered combination orbits, and demonstrate the sensitivity of recurrence strength to the spatial symmetry of the wave function imposed by the Pauli exclusion principle. Incorporation of an effective potential to model the influence of the exchange interaction in the semiclassical framework is in progress.

We are grateful to R. Jensen, V. Kondratovich, and J. Shaw for valuable discussions, to D. Cullinan and H. Flores for help in the lab, and special thanks to Sam Slishman.

[1] T. F. Gallagher, *Rydberg Atoms* (Cambridge University Press, Cambridge, England, 1994); *Rydberg States of Atoms and Molecules*, edited by R. F. Stebbings and F. B. Dunning (Cambridge University Press, Cambridge, England, 1983).
[2] J. Gao and J. B. Delos, Phys. Rev. A **49**, 869 (1994).
[3] P. A. Dando *et al.*, Phys. Rev. Lett. **74**, 1099 (1995); Phys. Rev. A **54**, 127 (1996).
[4] B. Hüpper *et al.*, Phys. Rev. Lett. **74**, 2650 (1995); Phys. Rev. A **53**, 744 (1996).
[5] M. Courtney *et al.*, Phys. Rev. Lett. **73**, 1340 (1994); Phys. Rev. Lett. **74**, 1538 (1995); M. Courtney *et al.*, Phys. Rev. A **51**, 3604 (1995).
[6] U. Eichmann *et al.*, Phys. Rev. Lett. **61**, 2438 (1988).
[7] H. A. Bethe and E. Salpeter, *Quantum Mechanics of One- and Two-Electron Atoms* (Plenum, New York, 1977).
[8] Levels were calculated using Ref. [7], with oscillator strengths from D. A. Harmin, Phys. Rev. A **24**, 2491 (1981).
[9] V. Kondratovich (private communication).
[10] P. A. Dando *et al.*, Phys. Rev. Lett. **80**, 2797 (1998).